Limnol. Oceanogr., 48(2), 2003, 632–646

Resolving phytoplankton photoprotective : photosynthetic carotenoid ratios on fine scales using in situ spectral absorption measurements

Lisa B. Eisner,[1] *Michael S. Twardowski,*[2] *and Timothy J. Cowles*
Oregon State University, College of Oceanic and Atmospheric Sciences, 104 Ocean Administration Building, Corvallis, Oregon 97330

Mary Jane Perry
University of Maine, School of Marine Science and Ira C. Darling Marine Center, 193 Clark's Cove Road, Walpole, Maine 04573-3307

Abstract

Temporal changes in phytoplankton pigments and spectral absorption were evaluated during June 1998 in East Sound, Orcas Island, Washington. High-resolution vertical profiles of in situ spectral absorption were obtained with a Wet Labs ac-9 (nine-wavelength absorption and beam attenuation meter), and pigment concentrations were determined for discrete water samples using high-performance liquid chromatography (HPLC). Fucoxanthin was the most abundant carotenoid, indicating the dominance of diatoms. We computed a slope index to evaluate changes in shapes of the in situ particulate absorption coefficient (a_p) spectra, a_p slope = $(a_p488 - a_p532)/(a_p676(488 - 532$ nm)). A clear linear relationship was seen between ratios of photoprotective : photosynthetic carotenoids (PPC : PSC) and these a_p slopes. While pigment package effects may alter the absorption spectra, in our data set we still found a significant relationship between pigment ratios and in situ a_p slopes. Retrieval of this relationship was facilitated by the low and relatively constant detrital absorption coefficient (a_d) values in our study area. Similar relationships were found between PPC : PSC ratios and the estimated phytoplankton absorption coefficient (a_{ph}) spectra. High PPC : PSC ratios and steeper a_p slopes were associated with high-light levels. Our results suggest that in situ absorption measurements can be used to estimate PPC : PSC ratios in areas where the a_d contribution is low or can be estimated. These variations in pigment ratios and spectral absorption reflect photoacclimation responses and/or changes in phytoplankton species composition and suggest in situ absorption measurements may be used to estimate pigmentation changes over fine temporal and spatial scales.

Rapid, in situ assessment of phytoplankton physiological condition has been a goal of plankton ecologists for many decades. The recent development and field use of multiwavelength biooptical instrumentation has brought us closer to that goal and provides the opportunity to quantify the relationship between in situ observations and traditional, discrete sample analyses of physiological condition. The work described in this paper was motivated by that opportunity and, in particular, tested the effectiveness of measurements of in situ absorption spectra as indicators of the photoadaptive state of the phytoplankton assemblage.

Pigments are widely used to characterize phytoplankton physiological state, species identity, and biomass in marine and freshwater environments (Falkowski and Raven 1997). Light harvesting pigments in the photosystem absorb light that impinges on chloroplasts within the cell. This absorbed light energy has three main fates, (1) carbon assimilation via photosynthesis, (2) dissipation as fluorescence, or (3) dissipation as heat. Photoprotective carotenoid (PPC) pigments help prevent damage to the chloroplast from excess light energy, while photosynthetic carotenoid (PSC) pigments are involved in transfer of energy to reaction centers during photosynthesis. Therefore, PPC : PSC ratios may serve as indicators of energy transfer pathways within phytoplankton cells.

Variations in the relative proportions of carotenoid accessory pigments also alter the shape of the phytoplankton absorption coefficient (a_{ph}) spectrum. Changes in the a_{ph} spectra have been used to differentiate low-light and high-light adapted cultures for a variety of different phytoplankton taxa (SooHoo et al. 1986; Johnsen et al. 1994). The slope of the a_{ph} spectra from 490 to 530 nm (normalized to 676 nm) has been found to be steeper in high-light compared to low-light adapted cultures (Johnsen et al. 1994). Such a_{ph} spectral variations are due to physiological changes in cellular pigment ratios and pigment packaging (intracellular self-shading; Duysens 1956). Under high light, increases in PPC, decreases in PSC, and a reduction in pigment packaging may cause the a_{ph} spectral slopes to become steeper, while the reverse

[1] Corresponding author (leisner@coas.oregonstate.edu).
[2] Present address: Department of Research, Wet Labs, Inc., P.O. Box 468, Saunderstown, Rhode Island 02874-0468.

Acknowledgments

This research was supported by an AASERT grant (N00014-96-10933) from the Office of Naval Research. Comments from Heidi M. Sosik and an anonymous reviewer substantially improved this manuscript. We thank Dian Gifford for assistance in water sample collection and for providing phytoplankton species data; Jan Rines for information concerning phytoplankton species; Chris Wingard and Russ Desiderio for help with data collection, data processing, and graphics; Andrew Barnard for spectral radiometer measurements; Van Holliday for help with sample collection; and Claudia Mengelt, Ricardo Letelier, and Margaret Sparrow for advice and support with HPLC analysis. Kathy Krogslund from the Marine Chemistry Laboratory at the University of Washington conducted nutrient analyses.

is true for low-light conditions. The in situ a_{ph} spectra also can reflect variations in taxonomic composition (Johnsen and Sakshaug 1996) and absorption by pigmented heterotrophic organisms.

Research over the past few decades has shown that changes in pigments and absorption coefficients, reflecting changes in phytoplankton physiology and species composition, are tied to fluctuations in the physical and chemical environment (irradiance, stratification, mixing, nutrients). Field studies have shown that variations in PPC and PSC potentially can be used to evaluate changes in light and mixing (Claustre et al. 1994; Moline 1998). In laboratory experiments, increases in the photoprotective pigments, diatoxanthin and diadinoxanthin, were associated with both increases in irradiance and decreases in nutrients (Latasa 1995).

These previous studies used discrete sample analyses to evaluate the photoadaptive state of specific samples. Common methodology for particulate absorption measurements (the quantitative filter technique, QFT, Yentsch 1962; Mitchell and Kiefer 1988), requires filtration of discrete water samples and analysis with a bench-top spectrophotometer to obtain a_p. The QFT allows estimation of the detrital absorption coefficient (a_d) following extraction of pigments from the filter (Kishino method, Kishino et al. 1985; Roesler 1992), thus providing an estimate of the phytoplankton absorption coefficient (a_{ph}). In contrast to this discrete sample analysis, the use of in situ multiwavelength optical instrumentation such as the Wet Labs ac-9 now allows the absorption coefficients for particulate (a_p) spectra to be estimated directly within the water column, enabling vertical profiles of $a_p(\lambda)$ to be easily obtained. Coupled with the measurement of phytoplankton pigment concentration using high-performance liquid chromatography (HPLC) on discrete samples, in situ absorption measurements now may provide a tool for assessing fine-scale variations in the photoadaptive state of phytoplankton. In addition, the nonintrusive nature of in situ optics provides an advantage over discrete water sample collection since one can eliminate the sampling artifacts during preservation, handling, and laboratory analysis. Finally, coincident measurements of physical parameters such as temperature (T) and salinity (S) allow a better correlation of biological and physical properties within the water column.

Our goals in this work were to determine the extent to which in situ a_p measurements can estimate phytoplankton accessory pigment composition over fine scales and to evaluate the resulting impacts on phytoplankton ecology at these scales. Specifically, we wished to (1) compare PPC and PSC concentrations from HPLC analyses of discrete water samples with in situ absorption spectra for estuarine phytoplankton assemblages, (2) demonstrate how in situ a_p and a_{ph} measurements can be used to evaluate PPC : PSC ratios over fine scales, (3) provide examples of the relationship of PPC : PSC ratios and absorption measurements to physical forcing mechanisms (light, nutrients, and mixing), and (4) quantify the potential effects of a_d and package effect variations on the relationship between PPC : PSC ratios and a_p and a_{ph} spectra.

Materials and methods

Sampling site—Data collection occurred from 14 to 24 June 1998 from the R/V *Henderson*, moored near the head of East Sound (148°40.62′N and 122°53.45′W), a fjord type inlet of Orcas Island, Washington (Fig. 1). The depth of the water column varied from 20 to 22 m depending on tidal stage.

In situ measurements of hydrography and biooptics—A vertical time series of temperature data (Fig. 2) was obtained with a thermistor chain located ~100 m east of the R/V *Henderson.* Vertical profiles of temperature, salinity, fluorescence, and spectral absorption were obtained with a free-falling optical instrument package. This package included a high-resolution conductivity–temperature–depth (CTD) sensor (SBE911, Seabird), a fluorometer (Wetstar, Wet Labs), and two nine-wavelength in situ spectral absorption and beam attenuation meters (ac-9, Wet Labs). A 0.2-μm filter (maxicapsule, Gelman) was attached to the intake port of one of the ac-9s to measure the absorption by dissolved materials. Wavelengths for in situ absorption measurements were 412, 440, 488, 510, 532, 555, 650, 676, 715 nm. The ac-9s were calibrated every 2–4 d during the study using the pure water calibration technique (Twardowski et al. 1999).

Collection of discrete water samples—Water samples were collected once or twice per day (Fig. 2) within and outside vertical intervals of high particle concentration. Samples for pigment composition, QFT absorption, nutrients, and phytoplankton taxonomy were either siphoned from depth, collected with a separate 5-liter Niskin bottle, or sampled with a rosette system of bottles (20 cm in height; 500-ml capacity) deployed with the optical instrumentation package. T and S signatures from CTD measurements were obtained for both water samples and in situ optical measurements and then used to match depths of water sample collection with optical measurements. Water samples and optical measurements were collected within 2.5 h of each other with the majority (80%) collected within 1 h.

Phytoplankton pigment analyses—For phytoplankton pigment determinations, water samples (0.5 to 1 liters) were filtered onto 25-mm glass fiber filters (GF/F filters, Whatman) and frozen in liquid N_2. Pigments were extracted overnight in cold 90% acetone, sonicated, and quantified using reverse-phase HPLC (Ultrasphere C18 column, dual wavelength SpectraSystem UV2000 absorption detector) following a modified mobile solvent protocol (Wright and Jeffrey 1997). Calibrations were done with external standards. Quantifiable pigments included chlorophylls (*a, b, c*1/*c*2), chlorophyllide *a,* PSC (19-hexanoyloxyfucoxanthin, 19-butanoyloxyfucoxanthin, fucoxanthin, peridinin), and PPC (alloxanthin, β carotene, diadinoxanthin, diatoxanthin, lutein/zeaxanthin, violaxanthin). To use chlorophyll *a* as a biomass reference level in pigment ratios, we computed the sum of chlorophyll *a* (Chl *a*) and chlorophyllide *a,* noted as Tchl *a.*

The output voltage of the Wetstar fluorometer on the profiling package was converted to Chl *a* equivalents using fluorometric analyses of extracted Chl *a* and pheopigments from

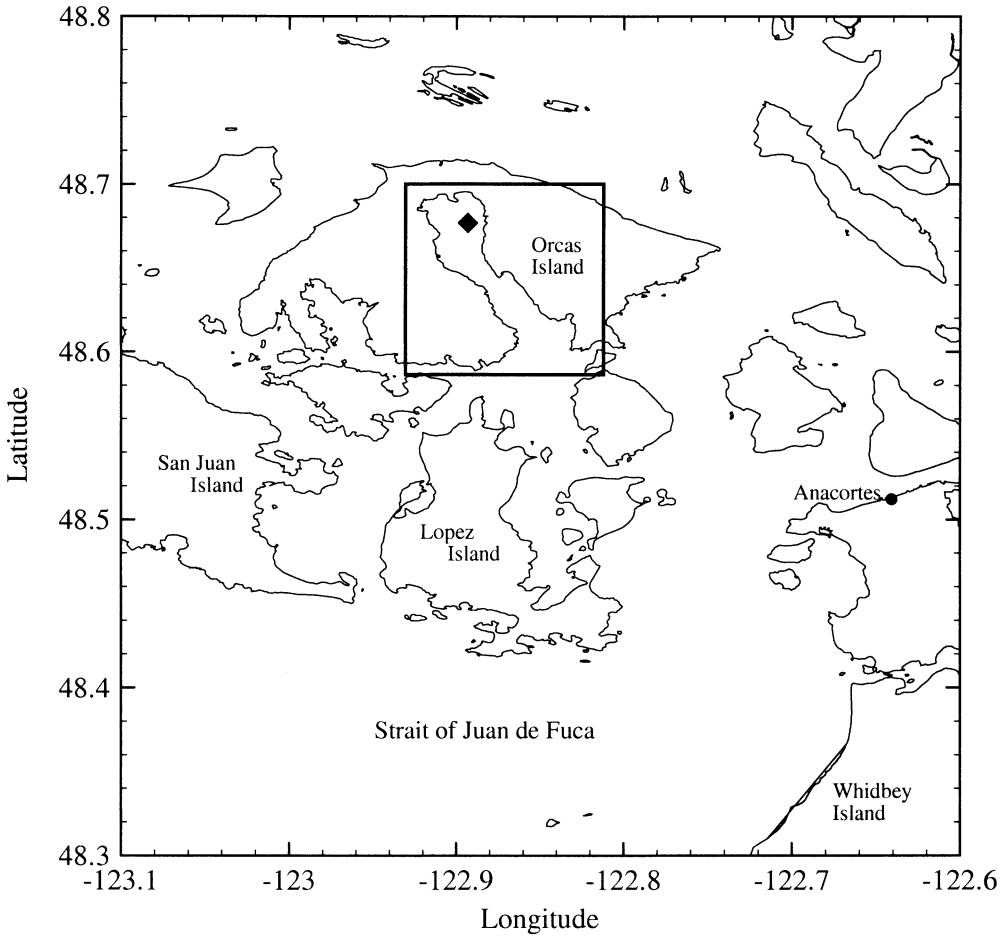

Fig. 1. Location of sampling site (R/V *Henderson*, black diamond) during June 1998 in East Sound, Orcas Island, Washington. East Sound marked by the square outline.

discrete water samples collected with the rosette sampler. Samples were filtered and extracted in cold 90% acetone and analyzed with a Turner Model AU-10 fluorometer (Parsons et al. 1984). Chl *a* concentration from extracted samples was linearly correlated with the in situ fluorometer voltage ($r^2 = 0.89$, $p < 0.0001$).

Discrete sample absorption spectra analyses—Discrete water sample a_p, a_{ph}, and a_d spectra were obtained following methods described in Culver and Perry (1999). A dual beam spectrophotometer (SLM-Amico DW2) was used to measure a_p spectra using the QFT (Yentsch 1962; Mitchell and Kiefer 1988). Phytoplankton pigments were removed using methanol (Kishino et al. 1985), and filters were rescanned to measure the a_d spectra. The a_{ph} spectra were determined by subtracting a_d from a_p spectra.

Nutrient analyses—Nutrient samples were immediately frozen after collection and analyzed within 6 months for total nitrate, nitrite, ammonium, phosphate, and silicate. Nutrient concentrations were determined with a Technicon autoanalyzer following standard colorimetry protocols (UNESCO 1994).

In situ particulate absorption spectra—The total in situ absorption coefficient (a_t) spectrum consists of absorption coefficients for water (a_w), particulates (a_p), and dissolved constituents (a_g). Pure water absorption is removed in the calibration methodology, so that the ac-9 measures $a_p + a_g$, denoted a_{pg}. Corrections for the temperature dependence of pure water absorption and variations in salinity were applied (Pegau et al. 1997), while the scattering error in our a_p measurements was removed by subtracting a_p715 nm from all wavelengths (Zaneveld et al. 1994). Data from the two ac-9s were used to estimate a_p by subtraction of a_g from a_{pg}. A time-lag correction for a slower flow rate was applied to the filtered ac-9 data in order to align the particulate and dissolved measurements.

Calculation of slopes from absorption spectra—To evaluate changes in the shape of the a_{ph} and a_p spectra from 488 to 532 nm, we normalized the absorption data to 676 nm. The slopes of the normalized absorption curves from 488 to 532 nm were computed:

$$a_x\text{slope} = \frac{(a_x488 - a_x532)}{(a_x676(488 - 532\ \text{nm}))}$$

where a_x is denoted as a_{ph} or a_p.

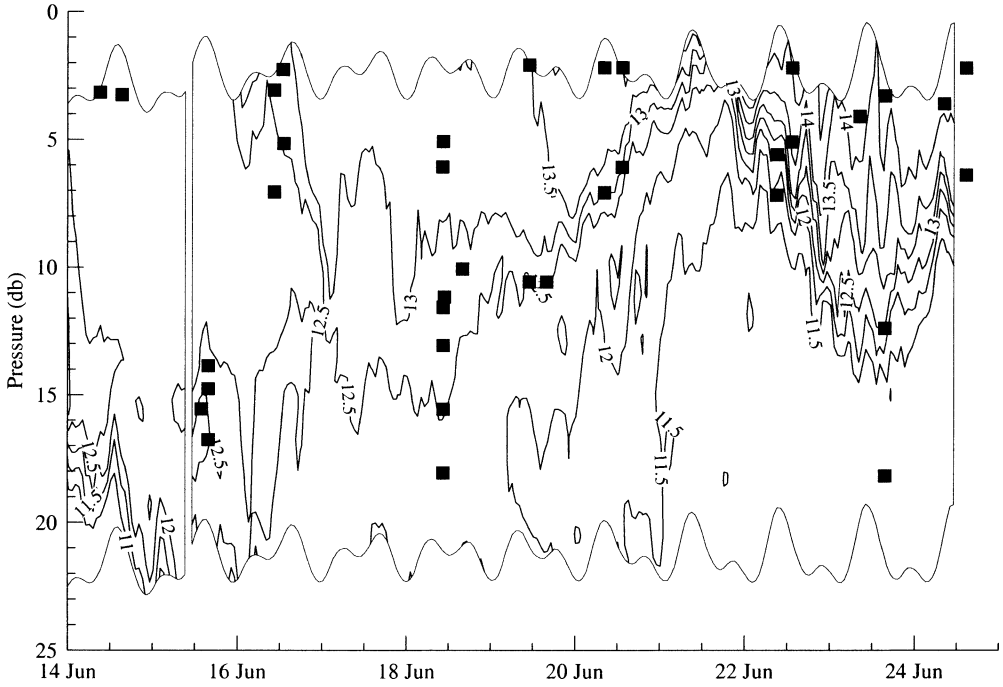

Fig. 2. Contour plot of thermistor chain data from mooring array for 14–24 June 1998, Pacific Daylight Time (PDT). The cyclic oscillations in thermistor sampling depths are due to tidal variations in water height. Black squares indicate depths of HPLC sample collection.

The ac-9 slope measurements were averaged over 1-m intervals (~50 data points at a profiler descent rate of 0.12 m s^{-1}). The a_{ph} and a_p slopes from the ac-9 and discrete samples were then compared to the PPC : PSC ratios from HPLC. A steeper slope was assumed to indicate an increase in relative amounts of PPC and/or a decrease in PSC based on the wavelength of maximum absorption and spectral shape of these pigment groups. The peak in vivo absorption for PPC is ~460 nm with specific absorption dropping near zero (0.001 m^2 mg^{-1}) at ~540 nm (Bidigare et al. 1990). In comparison, the peak in vivo absorption for PSC is ~490 nm, dropping near zero at ~590 nm. Chlorophyll *c* (Chl *c*) absorbs within the wavelengths of interest (488 to 532 nm), so absorption slopes also were compared to Chl *c* : PSC, Chl *c* : PPC, and Chl *c* : Tchl *a* ratios. We used model II linear regression analyses for all comparisons.

Detrital absorption (a_d) *estimation*—We investigated three methods to estimate and remove a_d from the ac-9 a_p measurements to obtain a_{ph}. Method 1 used the a_d results from specific discrete water samples collected close in time and depth to the ac-9 samples and analyzed with the QFT (and Kishino method). Method 2 used a mean a_d spectrum derived from all QFT data combined. Method 3 involved modeling the a_d shape and magnitude following methods in Roesler et al. (1989), using the equation

$$a_d(\lambda) = (a_d440)e^{(-s(\lambda-440))}$$

where $a_d440 = a_p440 - a_{ph}440$. We measured a_p440 with the ac-9 but needed to estimate $a_{ph}440$ and the exponent, *s*, to apply this method. We assumed that $a_{ph}676 \sim a_p676$ (since a_d decays exponentially from blue to red wavelengths, little detrital absorption is expected in the red region of the spectrum). We then assumed $a_{ph}440 = 1.61 \times a_p676$, where 1.61 was the mean blue : red value from QFT results. We used $s = 0.0065$ nm^{-1}, since it gave a_{ph} slopes insignificantly different from slopes found using QFT a_d from specific samples (95% CI for regression line slope, $s = 0.0060$ to 0.0072 nm^{-1}).

We then calculated ac-9 a_{ph} slopes based on the $a_{ph}(\lambda)$ that resulted from each of the three a_d correction methods outlined above. The linear regressions between a_{ph} slopes and PPC : PSC ratios were not significantly different using any of the methods ($p < 0.05$) after removal of one outlier (which had no comparable QFT data). For our data set consisting of ac-9 data and discrete pigment samples, we used the QFT a_d from specific discrete water samples (method 1) to calculate a_{ph} slopes for all samples, except for one outlier. Since QFT data were limited in number, some QFT a_d data were used for more than one ac-9/HPLC sample pair (QFT, $n = 21$; HPLC, $n = 35$, excluding outlier). For the single outlier and for fine-scale vertical profiles of ac-9 derived a_{ph} slopes, we used method 3 (or a variation of this method with a different *s*) to estimate a_d and subsequently a_{ph} slopes, since comparable QFT a_d data were unavailable, particularly for deep samples.

The relative importance of a_d to the a_p spectra was evaluated by comparing ratios of $a_p412 : a_p440$ from ac-9 measurements. Detritus has higher absorption at 412 nm than at 440 nm, while phytoplankton show the opposite trend. A ratio of $a_p412 : a_p440$ greater than 0.96 was assumed to indicate the presence of detritus, since QFT samples were never found to have $a_{ph}412 : a_{ph}440$ ratios exceeding 0.96. We used this indicator to identify depths within specific vertical

profiles that may have had high a_d relative to a_p, when discrete sample a_d data were unavailable.

Package effects—We examined the effects of packaging on our data set by reconstructing unpackaged a_{ph} spectra from phytoplankton pigment concentrations (determined by HPLC) using methods in Bidigare et al. (1990). We calculated the unpackaged phytoplankton absorption coefficient ($a'_{ph}(\lambda)$) from

$$a'_{ph}(\lambda) = \sum_{i=1}^{n} c_i a_i^*(\lambda)$$

where c_i is the concentration of pigment i (mg m^{-3}) and $a_i^*(\lambda)$ is the specific absorption coefficient of pigment i (m^2 mg^{-1}) at wavelength (λ). The percent loss of pigment absorption due to the package effect (Qa*, Morel and Bricaud 1981) can be calculated as in Nelson et al. (1993)

$$\text{Qa}^*(\lambda) = \frac{\text{measured } a_{ph} \text{ (includes packaging)}}{\text{reconstructed } a'_{ph} \text{ (unpackaged)}}$$

We used Qa*(676) to compare package effects. Absorption at 676 nm is due almost entirely to Tchl *a* and thus is not confounded by possible errors resulting from misidentified or missing pigments (phycobiliproteins) in the blue green region of the spectrum (Nelson et al. 1993).

Photosynthetically available radiation (PAR)—Irradiance measurements were obtained from a tethered spectral radiometer buoy (TSRB, Satlantic; *see* Cullen et al. 1997), deployed 30 m from the R/V *Henderson* from midmorning to late afternoon during 18–20 June and 22–24 June 1998. Downward irradiance (E_d) just above the surface was measured at 6 Hz at seven wavelengths (412, 443, 490, 555, 670, 684, 700 nm).

The $E_d(\lambda)$ from TSRB data was integrated from 400 to 715 nm to estimate PAR above the water surface. Subsurface irradiance was obtained using

$$E_d(z) = E_d(0)e^{-(Kd)z}$$

where $E_d(z)$ is the downward irradiance at depth z in meters, $E_d(0)$ is the downward irradiance just below the water surface, and K_d is the average vertical attenuation coefficient from 0 to z m. We assumed 5% loss of light at the air–water interface during calm conditions. $K_d(\lambda)$ was approximated by $K_E(\lambda)$, the vertical attenuation coefficient for net downward irradiance, where $K_E(\lambda) = a_t(\lambda)/\mu\text{bar}(\lambda)$, and $\mu\text{bar}(\lambda)$ is the average cosine for the light field. We used $a_t(\lambda)$ values estimated from ac-9 data and average mixed layer $\mu\text{bar}(\lambda)$ values from subsurface measurements made with a Satlantic SeaWiFS profiling multichannel spectral radiometer and an ac-9 from a nearby vessel in East Sound (A. Barnard pers. comm.). Subsurface PAR values were derived from the integral (400–715 nm) of estimated $E_d(z)$. To estimate prior light exposure, subsurface PAR values were averaged over the depth of mixing. Mixing was assumed to occur over a depth range that had a sigma–theta (density anomaly) differential <0.01 kg m^{-3}.

Results

Slopes of absorption spectra in relation to pigments—Clear linear relationships were found between PPC : PSC ratios and normalized a_{ph} and a_p slopes from ac-9 measurements ($r^2 = 0.93$, $p < 0.001$; Fig. 3a,c) and from QFT analysis of discrete samples ($r^2 = 0.81$ to 0.82, $p < 0.001$; Fig. 3b,d). The relationship between PPC : PSC ratios and ac-9 a_p slopes was robust throughout the entire range of values. There were only four data points in the higher (>0.5 g : g) PPC : PSC range; however, removal of these points did not significantly alter the linear regression ($p < 0.05$), but reduced the r^2 to 0.80. The PPC : PSC ratios for the entire HPLC data set (two replicates per sample) had coefficients of variation (CV) of 0.1 to 15.1% with a mean CV of 4.5% for all samples. For the colocated water parcels, ac-9 a_p slopes had CVs ranging from 20 to 76% with a mean CV of 40%. The derived ac-9 a_{ph} slopes had CVs ranging from 28 to 128% with a mean of 47%.

The regression line slopes and intercepts for a_{ph} and a_p slopes and PPC : PSC ratios were not significantly different from each other ($p < 0.05$) for either ac-9 derived data (Fig. 3a,c) or QFT data (Fig. 3b,d). These results suggest that detrital absorption had an insignificant effect on a_p slopes for our data set, with the exclusion of a single outlier (plus symbol in Fig. 3c). This conclusion was supported by the low a_d relative to a_p seen in QFT samples (Fig. 4).

For the outlier, we calculated a_d and subsequently the a_{ph} slope using a variation of the method 3 a_d correction (*see Methods*), assuming $s = 0.011$ nm^{-1}, since $s = 0.0065$ nm^{-1} (as applied to the other samples) did not yield a sufficient a_d correction. This higher s (steeper exponential slope) allowed the outlier sample point to fall close to the regression line for the PPC : PSC ratio and a_{ph} slope relationship (Fig. 3a). This single deep sample (18.1 m) from 23 June 1998 appeared to contain high a_d based on high ratios of a_p412 : a_p440 (1.12 for this outlier compared to a range of 0.87 to 1.03 for the other data points shown in regressions). This correction implies that the a_d shape and magnitude were different (steeper exponential slope and higher magnitude) for this outlier compared to the remaining samples (all but one collected at shallower depths).

Slopes compared to a_{ph} *ratios, Tchl* a, *and other pigment ratios*—We compared the ac-9 a_{ph} slope calculations and the more straightforward ratios of $a_{ph}488 : a_{ph}676$ and $a_{ph}488 : a_{ph}532$ and found that the PPC : PSC ratios had a stronger correlation with a_{ph} slopes ($r^2 = 0.93$) than with these a_{ph} ratios ($r^2 = 0.84$ and 0.70, respectively).

A comparison of Tchl *a* to a_p slopes showed that Tchl *a* had a much weaker relationship to a_p slopes than was found for PPC : PSC ratios ($r^2 = 0.45$ compared to 0.93). Removing the four lowest Tchl *a* values (and also steepest a_p slopes) from the analysis yielded an even weaker relationship ($r^2 = 0.20$). In contrast, strong linear relationships were found between ac-9 a_p slopes and ratios (g : g) of PPC : total pigments (chlorophylls, PSC, and PPC) and PPC : total carotenoids ($r^2 = 0.90$ and 0.93, respectively, $p < 0.001$). Weak linear relationships were seen between absorption slopes and ratios

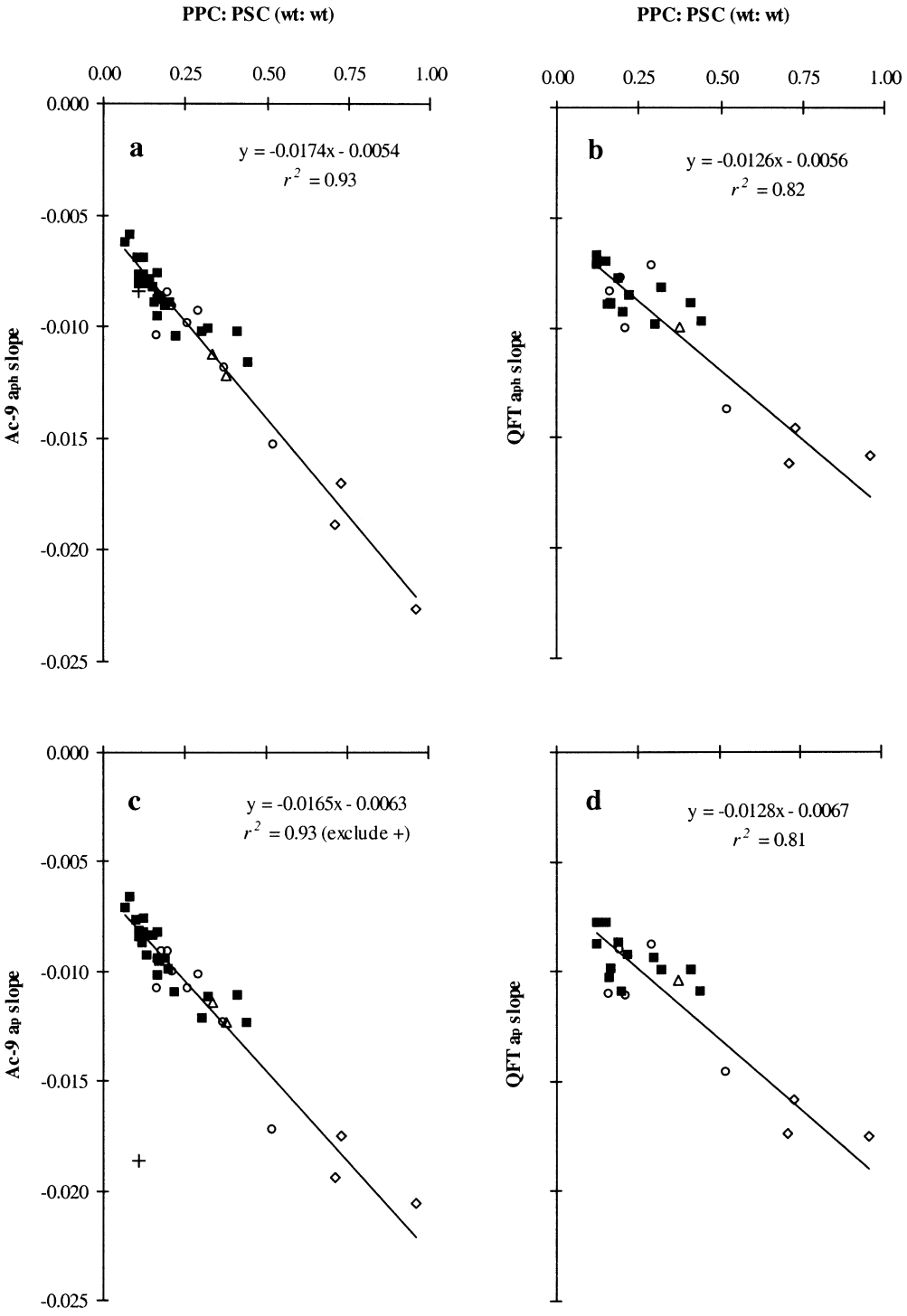

Fig. 3. Relationship of PPC : PSC ratios from HPLC analysis to normalized absorption slopes, slope = ($a488 - a532$)/($a676 \times (488 - 532$ nm)), from measurements of (a) in situ ac-9 phytoplankton absorption coefficients (a_{ph}), (b) discrete sample QFT a_{ph}, (c) in situ ac-9 particulate absorption coefficients (a_p), and (d) discrete sample QFT a_p. Open symbols are near surface samples (<5 m), and closed squares are deep samples (>5 m). Circles indicate surface mixed layer extends deeper than 5 m; diamonds indicate surface mixed layer <5 m; triangles indicate a continuously stratified surface layer. The plus sign (+) indicates a single outlier that appeared to contain high levels of detritus (*see text*). Model II linear regressions shown for $n = 36$ samples in panel a, $n = 35$ samples (excludes the outlier) in panel c, and $n = 21$ samples in panels b and d.

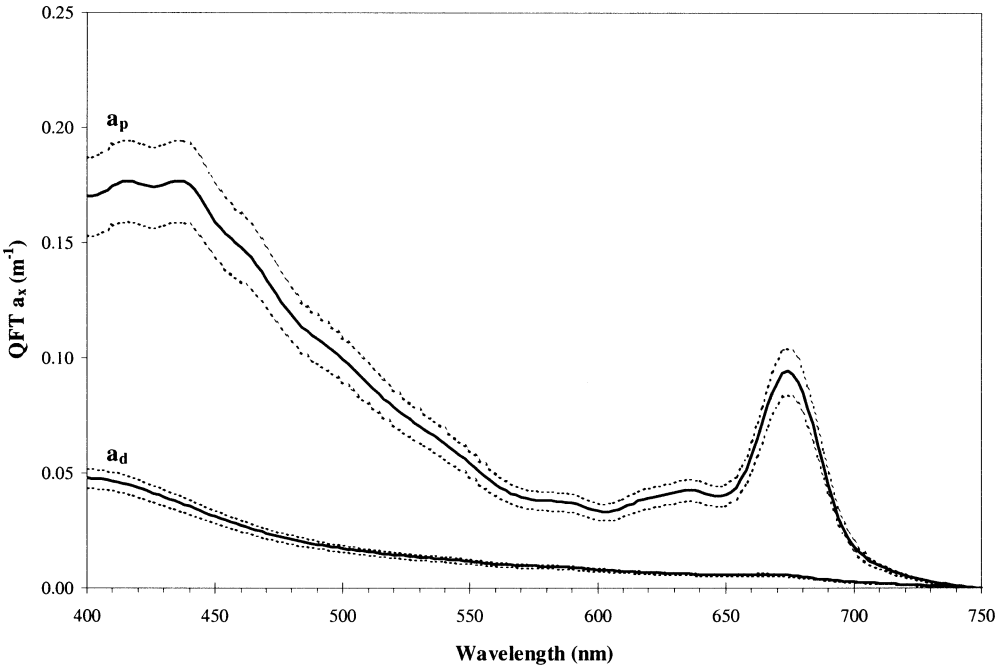

Fig. 4. Mean a_p and a_d spectra (solid lines) for QFT samples collected concurrently with HPLC samples, $n = 21$. Standard errors indicated by dashed lines.

(g : g) of Chl *c* : PSC, Chl *c* : PPC, or Chl *c* : Tchl *a* (r^2 = 0.12, 0.36, and 0.36, respectively).

Effects of a_d magnitude and shape on slopes—The ac-9 a_p data and subsequent a_p slope calculations are influenced by phytoplankton and detrital absorption. In other coastal and oceanic environments containing high and/or variable detritus concentrations, it is critical to understand how the a_p spectra are affected by variations in a_d magnitude and shape. These variations will in turn influence the relationship between a_p slopes and PPC : PSC ratios. To this end, we examined how variations in magnitude and shape (exponential slope, *s*) of a_d spectra might affect the relationship of ac-9 derived a_p slopes to PPC : PSC ratios. Specific sample a_d values (QFT data) were used for all analyses. We varied the a_d magnitude by multiplying a_d by 1, 2, 4, 6, 10, 20 (yielding $a_d412 : a_p412$ ratios of 0.21, 0.32, 0.50, 0.58, 0.70, 0.82, respectively) and added these a_d values to prior estimates of ac-9 a_{ph} values. We observed strong linear relationships between these new a_p slopes and PPC : PSC ratios up to $10a_d$ (r^2 = 0.88 and 0.71 for 4 and 10 a_d, respectively) (Fig. 5a). The linear relationship between a_p slopes and PPC : PSC ratios weakened at $20a_d$ (r^2 = 0.44, data not shown). The intercepts were significantly different ($p < 0.05$) than seen for the original ac-9 a_p regression for detrital additions greater than $4a_d$, while the slopes of the regression lines were not significantly different for any multiple of a_d.

We next varied the shape of the a_d spectra using a_d440 from each sample and s = 0.004, 0.006, 0.008, 0.010, 0.012 nm^{-1}, to obtain new a_p spectra (Roesler et al. 1989). A strong linear relationship was seen between the resulting a_p slopes and PPC : PSC ratios for all values of *s* (Fig. 5b). In this test, the slopes of the linear regression were significantly different ($p < 0.05$) from that seen for the original ac-9 a_p regression for $s \leq 0.005$ nm^{-1} and $s > 0.0125$ nm^{-1}. The intercepts were not significantly different.

Finally, we varied both the magnitude and shape (*s* values) of the a_d spectra. Magnitudes of 1 and 4 a_d and *s* values of 0.004, 0.012 nm^{-1} were used to calculate new a_d spectra for a_p slope estimates (Fig. 5c). Linear relationships between a_p slope and PPC : PSC ratios were found for all combinations of a_d magnitude and spectral shape, *s*. At the higher values of *s*, we observed greater differences in regression line intercepts between low and high a_d magnitudes.

The above analyses did not examine the effects of large variations in a_d between samples within one data set. We lacked the data to conduct such an analysis, but consideration of all points in Fig. 5c (as if the various a_d corrections were from a single data set) yields a linear association ($p < 0.001$, r^2 = 0.55) with significant differences in a_p slopes seen for PPC : PSC differences of 0.1 or greater (e.g., PPC : PSC ratios of 0.2 compared to 0.3, $p < 0.04$, two-sided *t*-test).

Effects of packaging on a_{ph} *slopes*—Package effects result from a combination of intracellular pigment (composition and concentration) and cell size variations. These variations can reduce the optical cross section of the cell and alter the a_p and a_{ph} spectra and slopes. Therefore, we attempted to quantify the effects of pigment packaging on a_{ph} slope variability.

Cell size (ranging from 0.6 to >50 μm diameter) can have an important influence on phytoplankton package effects between and within taxonomic groups (Morel and Bricaud 1981; Bricaud et al. 1983). The influence of cell size on packaging for diatoms was recently examined by Zinkel

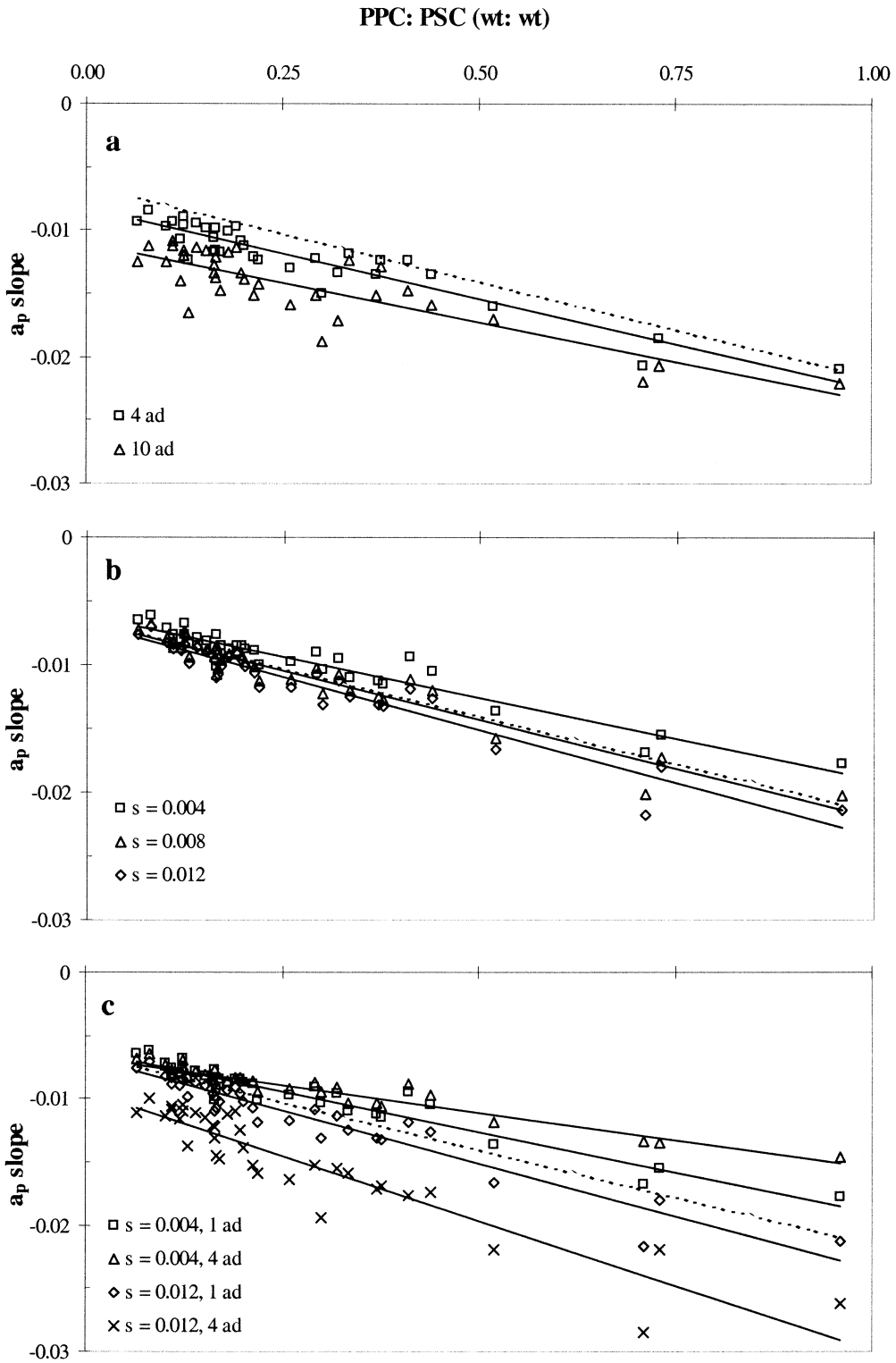

Fig. 5. Relationship of PPC : PSC ratios from HPLC analysis to a_p slopes derived by adding estimates of a_d to ac-9 a_{ph} values using (a) a_d magnitudes of 4 and 10 times measured a_d, (b) a_d spectral slopes, s, of 0.004, 0.008, 0.012, and (c) varying magnitudes and spectral shapes (s = 0.004 and 0.012 with 1 and 4 times measured a_d). Linear regression lines (solid lines) for varying a_d estimates are shown. Dashed lines show the linear regression of ac-9 a_p slopes as in Fig. 3a. a_p slope calculation as in Fig. 3.

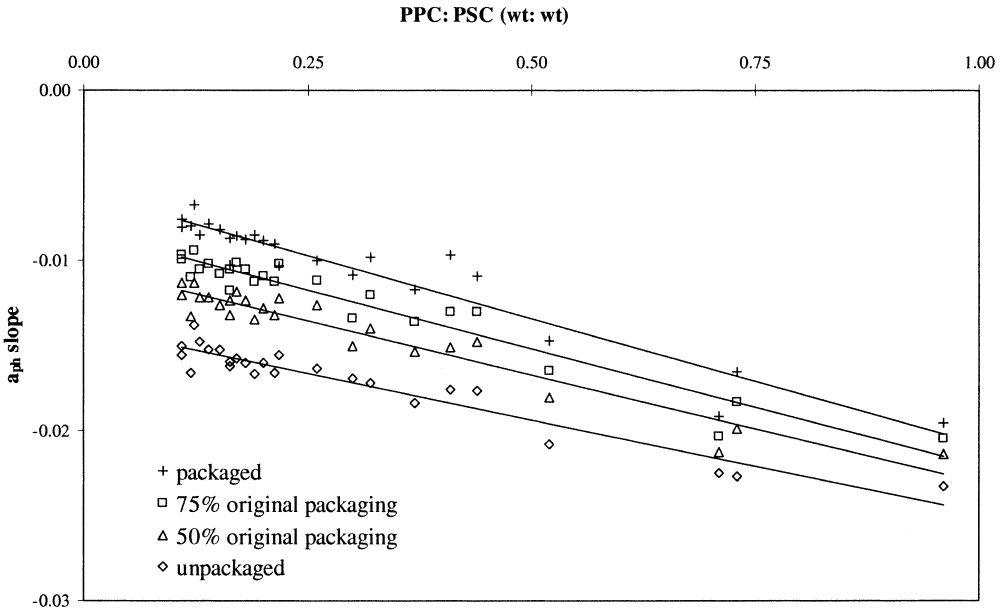

Fig. 6. Relationship of PPC : PSC ratios from HPLC analysis to a_{ph} slopes derived from HPLC data (as described in text) with varying amounts (0%, 50%, 75%, 100%) of packaging. Linear regression lines are shown (r^2 = 0.91 to 0.93). Data collected between 18 to 24 June 1998. a_{ph} slope calculation as in Fig. 3.

(2001), who found that, under low-light conditions (25 μmol photons m^{-2} s^{-1}), larger diatom species had increased packaging effects. To evaluate the potential impact of these cell size package effects on our a_{ph} slope method, we estimated a_{ph} slopes from the specific absorption coefficient data (a^*, m^2 mg Chl a^{-1}, Zinkel 2001, *see* her Fig. 2a) for small (n = 3) and large (n = 4) diatom species, assuming similar pigment composition for all species (Zinkel 2001). The resulting mean a_{ph} slopes were not significantly different for small compared to large diatoms ($p > 0.75$, mean slopes were -0.0073 and -0.0069 for small and large species, respectively). In this case, large size variations in diatoms (and presumed differences in packaging) did not significantly alter a_{ph} slope estimates.

Packaging effects for our data set were estimated using Qa*(676) derived from our QFT data. These Qa*(676) values ranged from 0.87 to 0.35 with a mean of 0.57. Qa*(676) values were significantly higher for surface depths (≤5 m) than for depths ≥10 m [mean Qa*(676) values of 0.59 compared to 0.44; t-test, $p < 0.05$], suggesting that cells located near the surface had less packaging than cells located at depth. The trends in Qa*(676) are similar for ac-9 derived Qa*(676) data. For comparison, Qa*(675) ranged from ~0.98 to 0.6 for a variety of diatom cultures reported in literature (Nelson et al. 1993). Bricaud et al. (1995) found Qa*(675) values of ~0.9 to <0.3 for samples with Tchl a ranging from 1.5 to 20 μg L^{-1} (overlapping the Tchl a range in our study), with Qa*(675) showing a general decrease with increasing Tchl a. We observed a weak trend of decreasing Qa*(676), with increasing Tchl a (although the scatter was large and the slope of the linear regression was not significantly different from zero). We found no significant relationships ($p > 0.05$) between Qa*(676) and a_{ph} slopes or PPC : PSC ratios.

Finally, we evaluated the variations in packaging on ac-9 a_{ph} slopes by comparing measured a_{ph} slopes to the a_{ph} slopes derived from a'_{ph} (unpackaged) data using varying percentages of packaging. The a_{ph} slopes with 0%, 50%, and 75% of their original packaging were on average 1.88, 1.48, and 1.25 times steeper than measured a_{ph} slopes ($p < 0.05$, t-tests, Fig. 6). A comparison of these ac-9 a_{ph} slopes to PPC : PSC ratios indicates that decreasing the package effect increases the magnitude of the regression line intercept but does not change the regression line slope appreciably. Similar results were obtained for reconstructed a_{ph} slopes derived from QFT data. We found linear relationships between a_{ph} slopes and PPC : PSC ratios for all packaging levels (r^2 = 0.91 to 0.93). As with the a_d evaluations, these analyses did not address the effects of large variations in packaging between samples within one data set (as may occur in many oceanographic regions). If all packaging variations are considered at once (as if the various package effects shown in Fig. 6 were from a single data set), a linear association between ac-9 a_{ph} slopes and PPC : PSC ratios is still found ($p < 0.001$; $r^2 = 0.54$).

Stratification, light, and nutrients—The thermistor chain record (Fig. 2) indicates that surface temperatures and mixed layer depths varied considerably over the 10-d survey period. Surface temperatures increased and surface mixed layers shoaled from 14 to 21 June 1998, with decreases in surface temperatures and deepening of surface mixed layers from 21 to 24 June 1998. Mean above surface PAR between 1000 and 1600 h was moderate on 18 June 1998 (800 μmol quanta

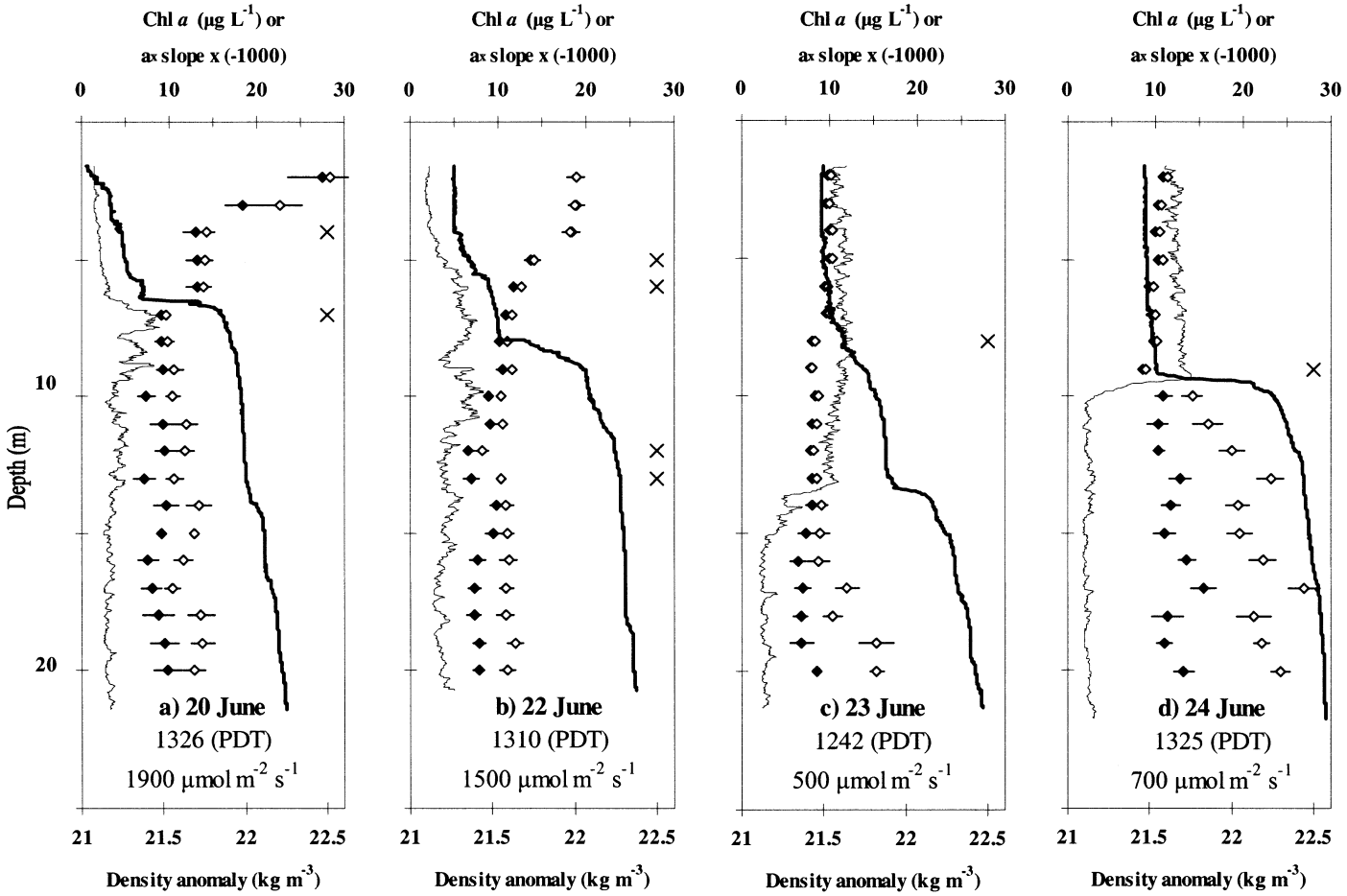

Fig. 7. Vertical profiles of density in sigma–theta (bold line), chlorophyll *a* calculated from in situ fluorescence (thin line), ac-9 a_p slopes (open diamonds), and a_{ph} slopes (closed diamonds) collected within a half hour of solar noon on (a) 20 June, (b) 22 June, (c) 23 June, and (d) 24 June 1998. The a_{ph} slopes were derived from ac-9 a_p data using the method 3 a_d correction (*see Methods text*) assuming $a_{ph}440 : a_{ph}676 = 1.61$ and an exponential slope, *s*, based on ac-9 $a_p412 : a_p440$ ratios. For samples with $a_p412 : a_p440$ ratios >0.96 (typically located below 10–15 m), we used $s = 0.011$ nm^{-1}. For all other samples we assumed $s = 0.0065$ nm^{-1}. The a_p and a_{ph} slopes were calculated as in Fig. 3 and multiplied by negative 1,000 for scaling purposes. Error bars on a_p and a_{ph} slopes indicate ±1 SE. a_p slopes that were significantly different (95% confidence level) from the 1-m interval directly above are indicated by an X. Significant differences were calculated only for depths with $a_p412 : a_p440$ ratio <0.96 (i.e., samples that did not appear to contain high levels of detritus). The mean PAR value for the hour prior to sample collection is displayed on each panel. Note the large changes in a_p and a_{ph} slopes in panels a and b compared to c and d.

m^{-2} s^{-1}), high on 19, 20, and 22 June 1998 (1,250, 1,450, and 1,550 µmol quanta m^{-2} s^{-1}, respectively) and low on 23 and 24 June 1998 (600 µmol quanta m^{-2} s^{-1}). Total N (nitrate N + ammonium N + nitrite N) in surface waters (<5 m) had minimum concentrations of 0.7, 2.1, 4.8, 1.6 µM and N : P ratios of 1.5, 3.0, 6.5, 4.0 on 20, 22, 23, 24 June 1998, respectively. Nitrogen was likely the limiting nutrient during this period, assuming Redfield ratios of 16 : 1 for N : P.

Vertical and temporal variations of a_p *slopes and pigment ratios*—Steeper a_p and a_{ph} slopes and higher PPC : PSC ratios were observed more often near the surface than at depth (Fig. 3). Vertical ac-9 profiles of a_p slopes and a_{ph} slopes were used to document fine-scale variations in PPC : PSC ratios (Fig. 7). Deeper in the water column (below the main pycnocline), the greater magnitude a_p slopes were likely due to higher a_d in these waters (based on $a_p412 : a_p440$ ratios). To estimate a_{ph} slopes, we derived a_d using method 3 (*see Methods*), with a slight variation for deep samples. We assumed that $s = 0.0065$ nm^{-1} in waters above the pycnocline with low a_d, and $s = 0.011$ nm^{-1} (as used for the single outlier) in deeper waters with high a_d (*see Fig. 7 legend*). These estimated a_{ph} slopes appear to be fairly low and constant below the pycnocline (with the possible exception of the 24 June profile), which suggests that PPC : PSC ratios were low and did not change appreciably in these deep waters. Note that these a_{ph} slope estimates are dependent on the assumptions made for a_d estimates (e.g., $s = 0.011$ nm^{-1} is an appropriate value for deep waters with high a_d).

The data from all four days (20, 22, 23, and 24 June 1998) show that a_p and a_{ph} slopes changed significantly at depths with large density gradients. For example, on 20 June 1998 (Fig. 7a), the a_p slopes were significantly steeper at 3 m than

4 m and at 6 m than 7 m (*t*-tests, $p < 0.002$). Both of these transitions occurred over large density steps. A prediction of PPC : PSC ratios from these ac-9 a_p slopes ($y = -55.43x - 0.292$, $r^2 = 0.94$, model 1 linear regression) suggests that the PPC : PSC ratios were twice as high at 3 m than 4 m (difference of 0.46 g : g) and at 6 m than 7 m (difference of 0.24 g : g). Taxonomic data collected on 20 June 1998 revealed greater variation in species composition across the pycnocline than seen within waters above or below the pycnocline (D. Gifford pers. comm.).

Temporal variations in a_p slopes and pigment ratios can also be seen in the profiles shown in Fig. 7. Surface a_p and a_{ph} slopes were steeper on 20 and 22 June relative to 23 and 24 June 1998. The higher irradiance levels and shallower surface mixed layer depths on 20 and 22 June (Figs. 2, 7) likely contributed to these slope differences between the dates. The 2-m phytoplankton populations, for example, were exposed to average irradiances four times higher on 20 and 22 June than on 23 and 24 June 1998 (~950 compared to ~250 μmol quanta m^{-2} s^{-1}).

Pigment ratios and a_p *slopes in relation to light*—We compared prior light exposures for samples collected between 1100 h and 1600 h to pigment ratios and a_p slopes. Positive associations were seen between mean PAR for the hour prior to sample collection and (diatoxanthin + diadinoxanthin) : PSC ratios, (diatoxanthin + diadinoxanthin) : (Tchl *a*) ratios, PPC : PSC ratios, and a_p slopes (linear regression $r^2 = 0.92$, 0.98, 0.96, and 0.94, respectively; Fig. 8). Similar but slightly weaker relationships to pigment ratios and a_p slopes were seen for PAR averaged over 30 min or 2 h prior to sample collection (data not shown). Since the TSRB was not deployed until ~4 h after dawn, we did not have enough data to adequately assess cumulative irradiance effects from the start of the light period.

Dominant phytoplankton species—The chemotaxonomic pigments with the highest concentrations were fucoxanthin, peridinin, and alloxanthin; these pigments were used to assess the relative abundances of diatoms, dinoflagellates, and cryptophytes (Jeffrey and Vesk 1997), respectively. The fucoxanthin : Tchl *a*, peridinin : Tchl *a*, and alloxanthin : Tchl *a* ratios indicate that taxonomic composition varied temporally and as a function of depth (Table 1). Fucoxanthin : Tchl *a* ratios were typically an order of magnitude higher than other biomarkers, which indicates that diatoms were the most abundant species (Table 1). *Chaetoceros socialis*, a colonial diatom, frequently was the most numerous diatom sampled, although its relative proportion of the assemblage varied over depth, time, and location within East Sound (D. Gifford, J. Rines pers. comm.).

Discussion

The key findings of this study were the strong relationships found between the ac-9 a_{ph} and a_p slopes and the HPLC-derived PPC : PSC ratios (Fig. 3). These relationships suggest that absorption measurements from in situ instrumentation may be used to estimate PPC : PSC ratios in field phytoplankton assemblages. The relationship between ac-9 a_p slopes and pigment ratios was robust in East Sound except in deeper waters where a_d was likely high. The general applicability of this approach in other coastal and oceanic waters, however, is dependent upon consideration of the contributions of detrital absorption (a_d), pigment packaging, species composition, and irradiance to the shape of the absorption spectrum at specific depths. For both the a_d and packaging sensitivity analyses, we were restricted by the narrow range of values in our particular data set. Analysis with a wider ranging data set that possesses larger variations in a_d and packaging would allow us to more fully evaluate the impact of these variations. In addition, a more extensive data set would permit us to address the combined effects of variations in a_d and packaging on the relationship of a_{ph} and a_p slopes to PPC : PSC ratios.

Our analysis of variable contributions of a_d to our estimated a_p slopes suggests that over a large range of a_d magnitudes ($a_d412 : a_p412$ up to 0.5) and spectral shapes (s from 0.004 to 0.012 calculated over 440 to 676 nm range, Fig. 5c) it is possible to infer PPC : PSC ratios from a_p slopes derived from in situ absorption measurements. Ideally, a_d values should be determined using the QFT for a representative number of samples. Measured, mean, or modeled (Roesler et al. 1989; Cleveland and Perry 1994) values of a_d can then be subtracted from the ac-9 a_p spectra to estimate a_{ph} values and slopes for samples collected within similar water masses. We suggest that in situ absorption measurements always be made with coincident measurements of water mass properties and the local light field to permit assignment of groups of a_p slopes to particular water mass types, thus reducing the impact of variable a_d magnitudes and spectral shapes on the interpretation of estimated PPC : PSC ratios.

Variation in pigment packaging may further complicate the interpretation of pigment ratios from absorption data (Hoepffner and Sathyendranath 1991). Within the data set we analyzed, we had a range of package effects [indicated by Qa*(676) of 0.35 to 0.9]. In spite of this variation, we were able to derive a clear linear relationship between PPC : PSC ratios and a_p and a_{ph} slopes. Our sensitivity analysis using a_{ph} data from the current study indicated that variable package effects can degrade the relationship between a_{ph} slopes and PPC : PSC ratios, if packaging varies while PPC : PSC ratios are held constant. In the natural environment, package effects may covary inversely with PPC : PSC ratios. For our data set, we found significantly higher package effects in deep than in surface samples, while PPC : PSC ratios were higher in the surface than at depth (although there was not a significant linear relationship between these two parameters). Since both decreases in packaging and increases in the PPC : PSC ratios can increase a_{ph} slopes (and vice versa), it will be necessary to evaluate the effects of both these factors on a_{ph} slopes to explain a_{ph} slope variability in other marine systems with a range of phytoplankton taxa. We suggest that estimates of HPLC-derived pigment concentrations and cell size (perhaps based on pigment biomarkers, Vidussi et al. 2001, or size fractionation of pigments) accompany in situ measurements of absorption to evaluate the effects of packaging on a_{ph} slopes.

Short-term temporal changes in a_{ph} slope may reflect pho-

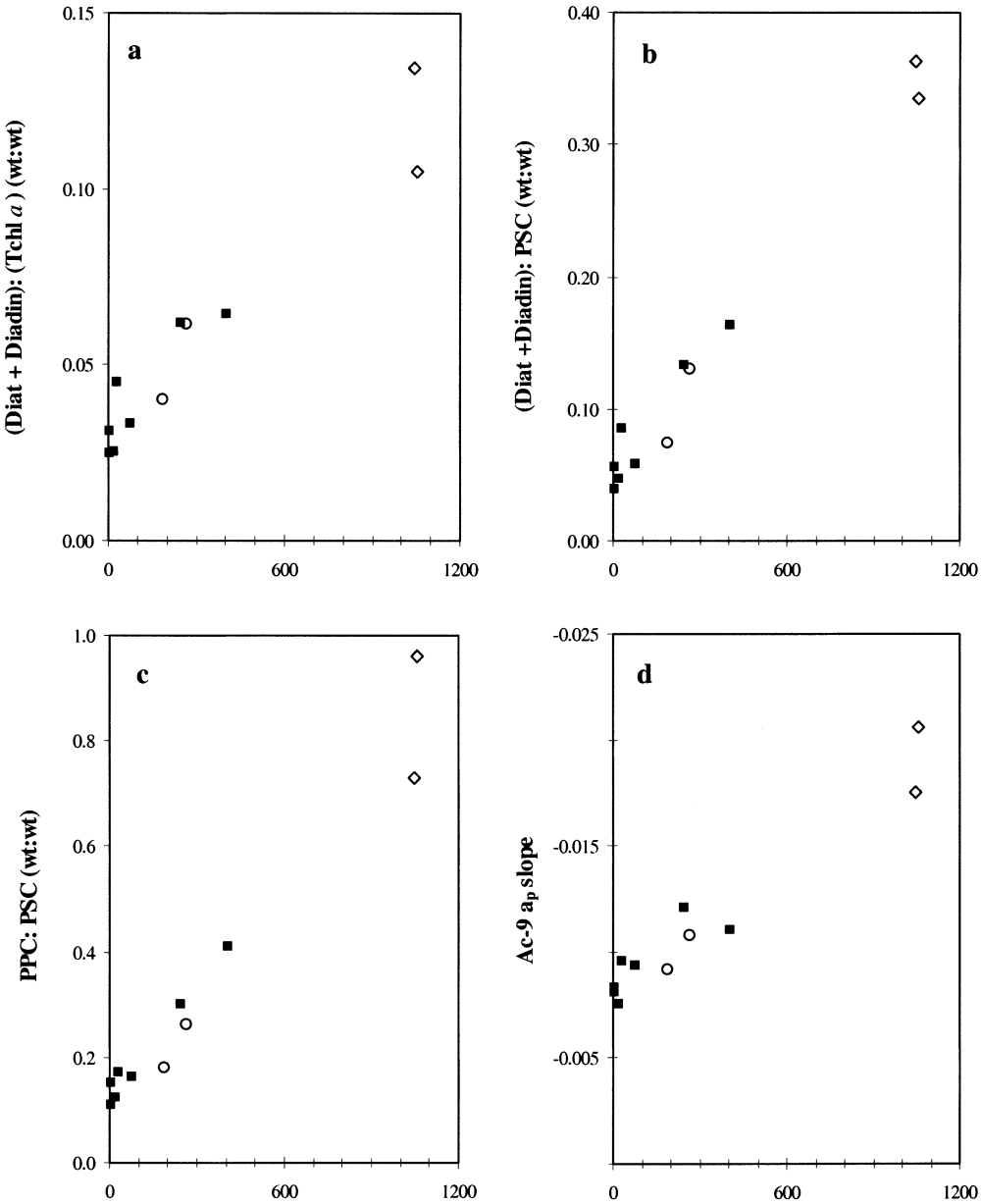

Fig. 8. Relationship of mean in-water PAR for the hour prior to sample collection to (a) (diatoxanthin + diadinoxanthin) : (Tchl *a*), (b) (diatoxanthin + diadinoxanthin) : PSC, (c) PPC : PSC, and (d) ac-9 a_p slopes. Samples collected between 1100 h and 1600 h Pacific Daylight Time on 18–20 June and 22–24 June 1998. PAR calculated as described in text. Symbols and a_p slope calculation as in Fig. 3.

toacclimation responses to variations in irradiance and provide clues to the light history of the phytoplankton community. If turnover (mixing) of the water column is slower than the time required for pigment synthesis, then indicators of photoacclimation such as (diatoxanthin + diadinoxanthin) : Chl *a* ratios can show a vertical gradient within the water column (Moline 1998). Culver and Perry (1999) found that natural phytoplankton from stratified depths in Puget Sound exhibited photoacclimation effects (photosynthetic pigment absorption coefficient : total phytoplankton absorption coefficient increased as irradiance decreased), while cells in mixed layers did not show a discernable photoacclimation trend. In our study, higher (diatoxanthin + diadinoxanthin) : Tchl *a* ratios and PPC : PSC ratios, steeper a_p and a_{ph} slopes, and higher prior (1 h) light exposures were seen in stratified surface waters than in deeper waters (Table 1, Fig. 8), which reflects the reduced vertical mixing associated with shallow stratification. Additional studies at intermediate- to high-light levels are required to quantify the time scales of response between irradiance, pigment ratios, and ac-9 a_p slopes and the intersection of these time scales with the longer time scales of species compositional changes within a water mass.

Variations in nutrient concentrations also can promote

Table 1. HPLC-determined pigment concentrations (μg L^{-1}) and ratios (wt : wt). Pigment types are abbreviated as follows: chlorophyll *a* + chlorophyllide *a* (Tchl *a*), chlorophyll *c*l/*c*2 (Chl *c*), fucoxanthin (Fuco), peridinin (Peri), alloxanthin (Allo), diatoxanthin + diadinoxanthin (DtDd), β carotene (Bcar), photoprotective carotenoids (PPC), photosynthetic carotenoids (PSC). Total pigment concentrations (total) were calculated as Tchl *a* + Chl *c* + PPC + PSC. Dates and times are Pacific Daylight Time. Samples >5 m shown in bold. Each data point represents the mean of two replicate samples unless indicated as no replicate (nr).

							PSC : Tchl *a*		PPC : Tchl *a*		
Date	Time	Depth (m)	Tchl *a*	Chl *c*	PP : PS	PP : total	Fuco : Tchl *a*	Peri : Tchl *a*	Allo : Tchl *a*	DtDd : Tchl *a*	Bcar : Tchl *a*
14 Jun	910	3.6	6.36	1.45	0.29	0.083	0.485	0.039	0.039	0.081	0.047
	1520	3.7	6.01	1.81	0.20	0.065	0.655	0.014	0.029	0.060	0.048
15 Jun	**1355**	**16.0**	**5.45**	**1.40**	**0.12**	**0.045**	**0.719**	**0.018**	**0.007**	**0.038**	**0.034**
	nr1551	**13.8**	**10.42**	**1.87**	**0.08**	**0.028**	**0.653**	**0.000**	**0.003**	**0.025**	**0.024**
	nr1551	**14.7**	**6.77**	**1.29**	**0.07**	**0.027**	**0.690**	**0.009**	**0.000**	**0.030**	**0.028**
	nr1551	**16.7**	**8.75**	**1.86**	**0.10**	**0.036**	**0.707**	**0.000**	**0.005**	**0.030**	**0.028**
16 Jun	1030	3.0	7.01	1.17	0.33	0.082	0.402	0.006	0.034	0.059	0.042
	1030	**7.0**	**12.73**	**2.75**	**0.16**	**0.055**	**0.598**	**0.027**	**0.013**	**0.046**	**0.034**
	1255	2.6	8.17	1.44	0.38	0.095	0.404	0.006	0.064	0.053	0.055
	1310	**5.6**	**8.92**	**2.29**	**0.17**	**0.057**	**0.658**	**0.020**	**0.020**	**0.052**	**0.035**
18 Jun	1030	5.0	6.47	1.14	0.37	0.094	0.386	0.038	0.048	0.052	0.055
	nr1030	**11.5**	**10.06**	**2.21**	**0.11**	**0.035**	**0.572**	**0.000**	**0.013**	**0.026**	**0.031**
	1030	**13.0**	**14.84**	**3.06**	**0.14**	**0.043**	**0.559**	**0.001**	**0.009**	**0.028**	**0.032**
	1030	**15.5**	**12.50**	**2.79**	**0.13**	**0.039**	**0.554**	**0.000**	**0.007**	**0.027**	**0.029**
	1030	**18.0**	**7.95**	**1.60**	**0.12**	**0.040**	**0.619**	**0.013**	**0.007**	**0.029**	**0.029**
	1020	**6.5**	**7.26**	**1.47**	**0.22**	**0.060**	**0.459**	**0.011**	**0.028**	**0.032**	**0.034**
	1053	**11.5**	**18.59**	**3.72**	**0.15**	**0.046**	**0.544**	**0.002**	**0.013**	**0.031**	**0.028**
	1600	**10.0**	**19.16**	**3.71**	**0.12**	**0.037**	**0.514**	**0.003**	**0.004**	**0.025**	**0.022**
19 Jun	1100	2.0	3.34	0.55	0.52	0.122	0.315	0.054	0.060	0.064	0.070
	1100	**10.5**	**10.96**	**2.16**	**0.19**	**0.058**	**0.529**	**0.013**	**0.024**	**0.034**	**0.036**
	1600	**10.5**	**9.92**	**2.19**	**0.16**	**0.050**	**0.553**	**0.007**	**0.014**	**0.033**	**0.029**
20 Jun	805	2.6	2.40	0.33	0.71	0.150	0.285	0.034	0.065	0.075	0.077
	820	**7.5**	**6.16**	**1.13**	**0.44**	**0.100**	**0.323**	**0.044**	**0.070**	**0.042**	**0.066**
	nr1333	2.5	1.62	0.23	0.96	0.170	0.262	0.037	0.096	0.105	0.060
	nr1322	**6.5**	**9.32**	**2.32**	**0.41**	**0.091**	**0.349**	**0.040**	**0.045**	**0.064**	**0.040**
22 Jun	**911**	**6.0**	**6.33**	**1.19**	**0.32**	**0.082**	**0.434**	**0.015**	**0.041**	**0.055**	**0.048**
	904	**7.6**	**6.03**	**1.30**	**0.20**	**0.058**	**0.499**	**0.000**	**0.028**	**0.031**	**0.045**
	1328	2.5	3.04	0.48	0.73	0.150	0.322	0.012	0.057	0.134	0.057
	1318	**5.4**	**6.21**	**1.31**	**0.30**	**0.076**	**0.434**	**0.020**	**0.028**	**0.062**	**0.039**
23 Jun	830	4.0	10.58	2.10	0.16	0.050	0.557	0.015	0.015	0.036	0.035
	1541	3.2	11.36	2.66	0.18	0.051	0.525	0.010	0.017	0.040	0.029
	1541	**12.3**	**12.03**	**2.84**	**0.11**	**0.034**	**0.617**	**0.000**	**0.006**	**0.025**	**0.025**
	1541	**18.1**	**2.05**	**0.41**	**0.11**	**0.039**	**0.711**	**0.000**	**0.004**	**0.036**	**0.029**
24 Jun	830	3.5	14.84	3.08	0.21	0.061	0.506	0.019	0.016	0.055	0.033
	nr1445	2.1	8.33	1.92	0.26	0.067	0.427	0.027	0.018	0.062	0.036
	nr1445	**6.3**	**10.31**	**2.82**	**0.17**	**0.048**	**0.527**	**0.000**	**0.009**	**0.045**	**0.031**

changes in physiology (Geider et al. 1993) and phytoplankton species succession that influence the relative pigment concentrations of the phytoplankton assemblage. However, the absence of an appreciable change in surface N levels, with the exception of 20 June 1998, suggests that for the most part, light influenced pigmentation more than nutrients during our study period.

Changes in PPC : PSC ratios can reflect physiological changes at the cellular level or indicate a shift in species composition with different light tolerances or nutrient requirements. During monospecific (or low species diversity) phytoplankton blooms, changes in the shape of the a_{ph} spectrum indicate physiological acclimation rather than taxonomic diversity. The phytoplankton assemblages in this study had differing species compositions (although diatoms were always the most abundant), photoacclimation responses, and/or light histories, all of which could influence a_{ph} slopes and pigment ratios. For example, the high PPC : PSC ratios and steep a_p and a_{ph} slopes seen in surface waters on 20 June 1998 likely resulted from photoacclimation as indicated by high diatoxanthin + diadinoxanthin : Tchl *a* ratios, in addition to taxonomic variation (presence of nondiatom species) as suggested by the relatively lower fucoxanthin : Tchl *a* ratios and relatively higher alloxanthin : Tchl *a*, peridinin : Tchl *a* ratios (Table 1).

Finally, our results indicate that in situ a_p slope measurements may reveal significant differences in estimated PPC : PSC ratios on vertical scales of ~1 m. This fine-scale resolution, obtained with free-fall deployment methods, also allows estimates of a_p slopes and pigment ratios to be directly compared with parameters such as temperature, salinity, density, and fluorescence measured over the same vertical scales. These sharp vertical gradients in biooptical properties are consistent with other observations of fine-scale plank-

tonic structure in East Sound (Dekshenieks et al. 2001; Rines et al. 2002; Alldredge et al. 2002), over the continental shelf (Cowles et al. 1993, 1998), and in the Baltic (Bjornsen and Nielsen 1991).

In conclusion, our results suggest that absorption measurements from in situ instrumentation can be used to estimate PPC : PSC ratios in field phytoplankton assemblages in areas with low detrital concentrations or where the a_d contribution can be adequately estimated. We show that the use of in situ optical instrumentation can provide a continuous vertical profile or temporal record of in-water optical properties, such as the normalized a_p spectral slope (488 to 532 nm), that can detect changes in pigmentation on finer scales than possible with conventional discrete water sampling methods. Pigmentation and in situ absorption changes were observed in response to changes in light and stratification, with increases in PPC : PSC ratios and a_p slopes associated with increases in irradiance and shoaling of the mixed layer. Such in situ–derived estimates of phytoplankton pigmentation changes may also provide insight into the recent light history of a particular phytoplankton population. For example, a time series of in situ absorption measurement could be used to estimate synthesis of PPC relative to PSC, given that advection effects are minimal or a single water mass can be monitored. While pigment package effects or a_d variations may alter the absorption spectra, in our data set we still found a significant relationship between pigment ratios and in situ a_p slopes. Further work is needed, however, to extend our understanding of the effects of packaging and a_d on the relationship developed in this study. With careful consideration of the range of factors influencing in situ absorption, these measurements can provide valuable information for deciphering the spatial, temporal, and physical factors driving photoacclimation and species diversity in field phytoplankton populations. We look forward to additional comparisons of in situ a_p, HPLC-derived pigment composition, and a_d estimates in other oceanic regions to confirm the general utility of a_{ph} and a_p slopes to estimate PPC : PSC ratios.

References

ALLDREDGE, A. L., AND OTHERS. 2002. Occurrence and mechanisms of formation of a dramatic thin layer of marine snow in a shallow Pacific fjord. Mar. Ecol. Prog. Ser. **233:** 1–12

BIDIGARE, R. R, M. E. ONDRUSEK, J. H. MORROW, AND D. E. KIEFER. 1990. In vivo absorption properties of algal pigments. SPIE Ocean Opt. X **1302:** 290–302.

BJORNSEN, P. K., AND T. G. NIELSEN. 1991. Decimeter scale heterogeneity in plankton during a pycnocline bloom of Gyrodinium aureolum. Mar. Ecol. Prog. Ser. **73:** 263–267.

BRICAUD, A., M. BABIN, A. MOREL, AND H. CLAUSTRE. 1995. Variability in the chlorophyll-specific absorption coefficients of natural phytoplankton: Analysis and parameterization. J. Geophys. Res. **100:** 13321–13332.

———, A. MOREL, AND L. PRIEUR. 1983. Optical efficiency factors of some phytoplankters. Limnol. Oceanogr. **28:** 816–832.

CLAUSTRE, H., P. KERHERVE, J. C. MARTY, AND L. PRIEUR. 1994. Phytoplankton photoadaption related to some frontal physical processes. J. Mar. Syst. **5:** 251–265.

CLEVELAND, J. S., AND M. J. PERRY. 1994. A model for partitioning absorption into phytoplanktonic and detrital components. Deep-Sea Res. I **41:** 197–221.

COWLES, T. J., R. A. DESIDERIO, AND M.-E. CARR. 1998. Small-scale planktonic structure: Persistence and trophic consequences. Oceanography **11:** 4–9

———, ———, AND S. NEUER. 1993. In situ characterization of phytoplankton from vertical profiles of fluorescence emission spectra. Mar. Biol. **115:** 217–222.

CULLEN, J. J., A. M. CIOTTI, R. F. DAVIS, AND M. L. LEWIS. 1997. Optical detection and assessment of algal blooms. Limnol. Oceanogr. **42:** 1223–1239.

CULVER, M. E., AND M. J. PERRY. 1999. The response of photosynthetic absorption coefficients to irradiance in culture and in tidally mixed estuarine waters. Limnol. Oceanogr. **44:** 24–36.

DEKSHENIEKS, M. M., P. L. DONAGHAY, J. M. SULLIVAN, J. E. RINES, T. R. OSBORN, AND M. S. TWARDOWSKI. 2001. Temporal and spatial occurrence of thin phytoplankton layers in relation to physical processes. Mar. Ecol. Prog. Ser. **223:** 61–71.

DUYSENS, L. N. M. 1956. The flattening of the absorption spectrum of suspensions, as compared to that of solutions. Biochim. Biophys. Acta. **19:** 1–12.

FALKOWSKI, P. G., AND J. A. RAVEN. 1997. Aquatic photosynthesis. Blackwell Science.

GEIDER, R. J., J. LA ROCHE, R. M. GREENE, AND M. OLAIZOLA. 1993. Response of the photosynthetic apparatus of *Phaeodactylum tricornutum* (Bacillariophyceae) to nitrate, phosphate, or iron starvation. J. Phycol. **29:** 755–766.

HOEPFFNER, N., AND S. SATHYENDRANATH. 1991. Effect of pigment composition on absorption properties of phytoplankton. Mar. Ecol. Prog. Ser. **73:** 11–23.

JEFFREY, S. W., AND M. VESK. 1997. Introduction to marine phytoplankton and their pigment signatures, p. 37–84. *In* S. W. Jeffrey, R. F. Mantoura, and S. W. Wright [eds.], Phytoplankton pigments in oceanography: Guidelines to modern methods. Unesco.

JOHNSEN, G., AND E. SAKSHAUG. 1996. Light harvesting in bloom-forming marine phytoplankton: Species-specificity and photoacclimation. Sci. Mar. **60:** 47–56.

———, O. SAMSET, L. GRANSKOG, AND E. SAKSHAUG. 1994. In vivo absorption characteristics in 10 classes of bloom-forming phytoplankton: Taxonomic characteristics and responses to photoadaptation by means of discriminate and HPLC analysis. Mar. Ecol. Prog. Ser. **105:** 149–157.

KISHINO, M., M. TAKAHASHI, N. OKAMI, AND S. ICHIMURA. 1985. Estimation of the spectral absorption coefficients of phytoplankton in the sea. Bull. Mar. Sci. **37:** 634–642.

LATASA, M. 1995. Pigment composition of *Heterocapsa* sp. and *Thalassiosira weissflogii* growing in batch cultures under different irradiances. Sci. Mar. **59:** 25–37.

MITCHELL, B. G., AND D. A. KIEFER. 1988. Chlorophyll *a* specific absorption and fluorescence excitation spectra for light-limited phytoplankton. Deep-Sea Res. **35:** 639–663.

MOLINE, M. A. 1998. Photoadaptive response during the development of a coastal Antarctic diatom bloom and relationship to water column stability. Limnol. Oceanogr. **43:** 146–153.

MOREL, A., AND A. BRICAUD. 1981. Theoretical results concerning light absorption in a discrete medium, and application to specific absorption of phytoplankton. Deep-Sea Res. **28A:** 1375–1393.

NELSON, N. B., B. B. PREZELIN, AND R. R. BIDIGARE. 1993. Phytoplankton light absorption and the package effect in California coastal waters. Mar. Ecol. Prog. Ser. **94:** 217–227.

PARSONS, T. R., Y. MAITA, AND C. M. LALLI. 1984. A manual of chemical and biological methods for seawater analysis. Pergamon.

PEGAU, W. S., D. GRAY, AND J. R. V. ZANEVELD. 1997. Absorption and attenuation of visible near-infrared light in water: Dependence on temperature and salinity. Appl. Opt. **36:** 6035–6046.

RINES, J. E. B., P. L. DONAGHAY, M. M. DEKSHENIEKS, J. M. SULLIVAN, AND M. S. TWARDOWSKI. 2002. Thin layers and camouflage: Hidden pseudo-nitzschia populations in a fjord in the San Juan Islands, Washington, USA. Mar. Ecol. Prog. Ser. **225:** 123–137.

ROESLER, C. S. 1992. The determination of in situ phytoplankton spectral absorption coefficients: Direct measurements, modeled estimates, and applications to bio-optical modeling. Ph.D. dissertation, Univ. of Washington, Seattle.

———, M. J. PERRY, AND K. L. CARDER. 1989. Modeling in situ phytoplankton absorption form total absorption spectra in productive inland marine waters. Limnol. Oceanogr. **34:** 1510–1523.

SOOHOO, J. B., D. A. KIEFER, D. J. COLLINS, AND I. S. MCDERMID. 1986. In vivo fluorescence excitation and absorption spectra of marine phytoplankton: I. Taxonomic characteristics and responses to photoadaptation. J. Plankton Res. **8:** 197–214.

TWARDOWSKI, M. S., J. M. SULLIVAN, P. L. DONAGHAY, AND J. R. V. ZANEVELD. 1999. Microscale quantification of the absorption by dissolved and particulate material in coastal waters with an ac-9. J. Atmos. Ocean. Technol. **16:** 691–707.

UNESCO. 1994. Protocols for the Joint Global Ocean Flux Study (JGOFS) core measurements. IOC Manual and Guides, **29.**

VIDUSSI, F., H. CLAUSTRE, B. B. MANCA, A. LUCHETTA, AND J. MARTY. 2001. Phytoplankton pigment distribution in relation to upper thermocline circulation in the eastern Mediterranean Sea during winter. J. Geophys. Res. **106:** 19,939–19,956.

WRIGHT, S. W., AND S. W. JEFFREY. 1997. High-resolution HPLC system for chlorophylls and carotenoids of marine phytoplankton, p. 327–341. *In* S. W. Jeffrey, R. F. Mantoura, and S. W. Wright [eds.], Phytoplankton pigments in oceanography: Guidelines to modern methods. Unesco.

YENTSCH, C. S. 1962. Measurement of visible light absorption by particulate matter in the ocean. Limnol. Oceanogr. **7:** 207–217.

ZANEVELD, J. R. V., J. C. KITCHEN, AND C. C. MOORE. 1994. Scattering error correction of reflecting tube absorption meters. Proc. SPIE Int. Soc. Opt. Eng. **12:** 44–55.

ZINKEL, Z. V. 2001. Light absorption and size scaling of light-limited metabolism in marine diatoms. Limnol. Oceanogr. **46:** 86–94.

Received: 17 December 2001
Accepted: 5 November 2002
Amended: 7 November 2002